X-661-72-447
PREPRINT

NASA TM X- 66136

RESULTS ON THE ENERGY DEPENDENCE OF COSMIC RAY CHARGE COMPOSITION

V. K. BALASUBRAHMANYAN
J. F. ORMES

DECEMBER 1972
REVISED MAY 1973

GSFC — GODDARD SPACE FLIGHT CENTER
GREENBELT, MARYLAND

/

RESULTS ON THE ENERGY DEPENDENCE OF COSMIC RAY CHARGE COMPOSITION

V. K. Balasubrahmanyan and J. F. Ormes
Goddard Space Flight Center, Greenbelt, Maryland 20771

ABSTRACT

Measurements using a balloon borne ionization spectrometer on the differential energy spectra of the heavy nuclei of the galactic cosmic radiation are reported. The results include more data and improved charge and energy analysis over our previously reported results. The spectra of individual elements up to oxygen and groups of nuclei up through iron have been measured up to almost 100 GeV/nucleon. The energy spectrum of the secondary nuclei, B+N, is steeper than that of the primary nuclei, C+O, by $\gamma = 0.21 \pm .09$ in agreement with Smith et al., 1973. The spectral shapes found by us are reasonably well represented by single power laws between 2 and 60 GeV/nucleon. Our data are consistent with the decrease in the secondary to primary ratio found by Juliusson et al. (1972) above 20 GeV/nucleon, but our data show no evidence for any sudden change in this ratio within counting statistics. The most dramatic finding is that the spectrum of the iron nuclei is flatter than that of the carbon and oxygen nuclei by 0.57 ± 0.14 of a power. The $10 \leq Z \leq 14$ group spectrum is consistent with that of C+O within errors. The experimental techniques for charge and energy determination are presented. Charge resolution is unique through oxygen, and at iron the error is $\pm$ one charge, so the charge groups are clearly separable. Energy is measured with $\sigma = 30\%$ between 2.5 and 25 GeV/nucleon. Corrections due to nuclear disintegration and losses of energy out the bottom of the spectrometer are discussed.

I. INTRODUCTION

Until recently the detailed study of the energy distribution of galactic cosmic rays above 10 GeV/nucleon was confined to integral measurements using threshold devices (von Rosenvinge, 1970, Webber et al., 1973). Current experimental programs of the Berkeley group (Smith et al., 1973), University of Chicago (Juliusson et al., 1972) and Goddard Space Flight Center (Ormes and Balasubrahmanyan, 1970) are attempting to extend the knowledge of charge composition to approximately 100 GeV/nucleon. For the first time differential measurements of the energy spectra of individual charges and charge groups above 10-GeV/nucleon are being reported (Ormes et al., 1971, and Smith et al., 1973). The new results in this energy region point towards very significant developments in our understanding of the life history of cosmic rays. Below a few GeV most of the experimental results were consistent with an energy independent composition. After a thorough analysis in which an improved charge resolution was coupled with detailed trajectory and energy analysis, we conclude that the cosmic ray composition varies with energy above 1 GeV/nucleon. This will have important implications for cosmic ray astrophysics. It is only by studying all of the relevant indicators, the secondary/primary ratio, the spectral exponents of the various primary components, and the secondaries from iron, that we can understand cosmic ray acceleration and propagation in a self consistent manner. We believe that with these measurements now being reported we can begin to separate acceleration and propagation effects and that this represents an important step forward in cosmic ray research.

In this paper our results on high energy composition are presented and their implications are discussed. The preliminary analysis presented earlier (Ormes et al., 1971, hereafter called OBR) was not sufficiently detailed or sophisticated to reveal all of these spectral differences. The results we present here are greatly improved by the use of a multidimensional charge analysis with more efficient background rejection, and a more accurate energy determination. Complex couplings between the charge, energy and trajectory information have been taken into account and will be discussed.

II. EXPERIMENTAL DETAILS

The balloon-borne instrument shown in figure 1, consisted of three major components, a charge measuring module, a spark chamber for determining particle trajectories, and an ionization spectrometer for measuring total energy. The charge of an incoming particle was determined using two plastic scintillators, a Lucite Cerenkov counter, and a CsI mosaic. Each detector had a sensitive area of 50 cm x 50 cm. The spark chamber was a digitized wire to wire chamber with four perpendicularly oriented planes, each with 200 wires spanning 50 cm. For each particle four (x,y) measurements were available. The trajectory from the spark chamber was used to eliminate the dispersion in pulse height due to the variation of response over the area of the detector and due to the angle of incidence of the particles. A discussion of these corrections and details of the instrumentation have been presented previously (Ormes and Balasubrahmanyan, 1970.)

The charge-module was followed by an electron cascade section consisting of a sandwich containing 12 tungsten plates and plastic scintillators.

This section was designed to separate electrons from protons, and its thickness was 11 radiation lengths or about 1/2 a proton interaction mean free path (mfp). Results on the electron component are being published separately (Silverberg et al., 1973). The electron cascade section was followed by a nuclear cascade section consisting of 7 modules of iron, each 1/2 mfp thick. Each module had three plastic scintillators uniformly distributed inside the iron and viewed by a single photomultiplier tube at each of two opposite ends. Since a sample of the number of particles in the cascade was taken every 1.5 radiation lengths, the fluctuations due to low energy electron cascades were minimized. All the 23 detectors were pulse height analyzed and had dynamic ranges of 10^4.

The payload weighed 6000 lbs and it was flown on a mylar scrim balloon of 26 x 10^6 ft^3 volume from Holloman Air Force Base in southern New Mexico on November 11, 1970. Useful data was obtained at a ceiling altitude of 7.4 gm/cm^2 for 14.4 hours. The geometric factor for the data presented was 725 cm^2 ster and the live time was 21.7 x 10^3 sec. Particles at zenith angles greater than 25° were excluded, yielding a total exposure factor of 1420 cm^2 ster sec.

III. CHARGE DETERMINATION & BACKGROUND REJECTION

The charge analysis is extremely critical because of its coupling with the energy determination and because of the background problems. As we shall see below, the response of the spectrometer depends upon energy/nucleon, and in order for this to be determined from the total observed energy deposit, the mass of the particles must be known. Furthermore, below about 2 GeV/nucleon, the Cerenkov (C) response is energy dependent, and so

the charge analysis depends upon the energy/nucleon. An interative procedure is followed. First the charge is determined assuming that the C response is energy independent. From the charge a mass is assumed, and energy is determined. This energy is used to correct the predicted C response and the charge determination is rechecked. If it shifts, then the energy is redetermined. The scintillators at low energy show a slight increase due to the inverse square dependence of ionization loss on velocity, but since the effect is less than 5%, no correction was made.

We consider first the details of the charge measurement.

The charge was measured by the four detectors of the charge module. The unique identification of a charge and the rejection of background depended upon two factors. The charge as measured by all four detectors had to be consistent within errors, and the trajectory of the particle had to be well defined and lie within the telescope geometry. When these conditions were met, pulse heights were corrected for geometrical variations in response using the trajectory data.

Since the study included singly charged particles and iron nuclei as well as the light and medium nuclei, the tracks of the incident particles had to be determined over an ionization range of more than 600. With the knock-on probability increasing as Z^2, heavier nuclei were invariably accompanied by knock-on electrons which caused confusion in determining the track. A computer algorithm was developed which detected the tracks of heavy ($Z \geq 3$) nuclei with an efficiency estimated as 95%.

Since the probability of a spark not forming along the track of the heavy nucleus was negligible, the main problem was to pick the correct trajectory

from a number of possible trajectories. The algorithm tried to fit straight trajectories through all combinations of sparks in the four decks of the wire grid spark chamber. The best fit to a straight line was selected with extra weighting given to sparks in which more than one adjacent wire participated. The mean number of sparks per event per plane increased from about 2.5 at helium to about 5 at neon. This saturated the multiple sparking efficiency of the chamber and so above neon there was no continuing increase in the number of sparks due to delta rays. By selecting tracks for the presence of sparks in which 2 or more wires participated, most of the possible spurious tracks were eliminated. The trajectories determined by this algorithm were projected to their exit point in the iron spectrometer and were found highly correlated with sudden drops in the module signals. We conclude that "chamber inefficiency" is not a cause of missing a track, but the delta rays lead to some uncertainty in track location. In order to check that this is not a problem, the zenith angle distributions of all nuclei have been checked to see that they correspond to expected distributions. If angular inaccuracies were more than a few degrees, the distributions would be broadened, and this was not observed. From this we estimate that $\sigma \leq 2^\circ$ for the zenith angle measurements.

Our confidence in the tracks is further enhanced because we have subsequently flown an experiment in which the number of decks was increased form 4 to 8. From an analysis of this new data it is clear that the trajectories picked by the 4 deck algorithm correspond closely to the 8 deck tracks.

TABLE 1

Criteria for Selecting Simple Events:

1. PARTICLE TRAJECTORY INTERSECTS COINCIDENCE SCINTILLATORS
2. ALL 4 PLANES CONTAIN SPARKS
3. LEAST SQUARES FIT OF DATA TO STRAIGHT LINE <1.5 WIRES
4. THERE IS NO SECOND TRAJECTORY IN THE CHAMBER SATISFYING 1, 2 AND 3 ABOVE WHICH HAS A DIFFERENT ZENITH ANGLE ($> 5°$) AND/OR POSITION (> 0.5in)

Following the algorithm, events were divided into two classes, called simple and complex. Simple events had a single trajectory which passed all of the tests listed in table 1. The failure of any one would have classified it as complex. Only simple events were used in the analysis, and possible errors introduced by this procedure will be discussed below.

The selection of simple events served to eliminate a large fraction of the background events. These background events were most abundant at Li and fell off rapidly with increasing charge. In particular, the spark chamber removed both atmospheric showers which could pass through the charge module unaltered and events caused by interactions in the spectrometer which triggered the experiment with back-scattered particles. The remaining background is eliminated by the charge determination procedure.

To obtain the charge, the raw pulse heights were corrected for analyzer non-linearities and for zenith angle and spatial variations in response. Due to the dispersions in the detectors, the observed pulse heights were distributed around the centroids characteristic of each charge in the four dimensional representation. Single and two dimensional pulse height

distributions were constructed from corrected pulse heights, and the centroid and resolution were found for each charge and for each detector. A distance of each event from the charge centroid was determined by calculating the root mean square distance from the centroids in units of the resolution for the appropriate charge. For each particle, the charge was assigned from the centroid which gave the minimum distance. Particles were rejected if their average distance was more than about FWHM/2 away from the centroid. The correction for particles lost in this selection procedure will be discussed below.

In order to demonstrate the selectivity of the method, a one dimensional charge distribution was constructed. A charge was determined as the minimum in the parabola formed by the distance to the three closest centroids. (If for example, an oxygen nucleus passed through two detectors, lost a proton and became a nitrogen, its distance to the oxygen and nitrogen centroids would be minimized and its charge from the parabola fit would be approximately 7.5.) The charge histogram for charges 3 to 8 shown in figure 2 was constructed in this manner. This analysis has greatly improved the signal to noise ratio of the data over the earlier analysis (OBR) in which only two detectors were used for charge identification.

Individual charges are well resolved. The good peak to valley ratio shows that background rejection has been quite effective. In the iron range of the spectrum $\Delta Z = \pm 1$ charge unit, and so iron is separated from its fragmentation products. By far the most background exists in the Li and Be region, which is characteristic of experiments deep in the atmosphere, and so for these elements the spectra are likely to still have background

contamination. The problem is that atmospheric showers from proton or helium interactions can produce 9 particles which in turn can pass through the charge module in a closely collimated bunch. Since the charge module contains only 0.16 radiation lengths of material, little cascade development takes place there and so the shower often passes through the charge module essentially unaltered.

Let us consider the effects of the background rejection. In order to insure that background is minimized, strict criteria have been placed on the consistency of the pulse height measurements. This may mean that some events, especially those which interact near the top of the spectrometer and produce backscatter, may be rejected. It is believed that this affects the acceptance of nuclei in the range of the light and medium nuclei, because the backscattered energy can be some 10 or 20 times minimum. However, this probably does not affect the heavier nuclei. It is difficult to identify these events in the data. Pulse heights are either totally inconsistent or the spark chamber trajectory is complex and a track cannot be found. Events which lie outside the error range but which have simple tracks could represent at most a 20% correction to the data. The point at which this final cut (FWHM/2) is taken is such that the L/M ratio and the individual charge composition agrees with the published literature. Under these conditions, we do not believe our spectra for B and all higher charges are affected by background contamination. However, good events are undoubtedly rejected by our strict criteria. This problem will be the subject of further study, both with more detailed analysis and with an improved version of the spark chamber in which multiple trajectories

can be seen.

To check that the spark chamber event classification scheme was not by itself biasing the data we analyzed all the complex events assuming they had trajectories at the most probable response angle of the telescope. To select these events they were required to deposit energy in the spectrometer modules so that their zenith angles probably did not exceed 25°. These data were then subjected to the same charge analysis as used for the simple events. The data for all the classifications of complex events listed in table 1 were consistent with being background. It is interesting to note that the number of "iron" group nuclei identified as complex is consistent with the expected number of interactions of iron nuclei in the charge module. For carbon nuclei, an upper limit of 18% can be put on the losses to well identified complex events and to 25% if marginally identified nuclei are allowed. The most probable correction is in the range of 5 to 10%. As discussed above, many carbon induced background events may be complex, but they do not appear to have consistent pulse height measurements. We do not believe that this is due to delta rays in the chamber but due to interactions in the material of the spectrometer.

IV. ENERGY MEASUREMENT

The incident nuclei interacted in the ionization spectrometer and dissipated their energy via nuclear and electron cascades from π^0 decay. The light signal seen by the photomultiplier tubes in the spectrometer was related to the energy of the incident nucleus (Murzin, 1971, Akimov et al., 1970, and Jones et al., 1969.)

Most of the incident heavy nuclei interacted in the tungsten module,

and so a first approximation to the energy of the incident particles was obtained by taking the sum over all the modules of the number of equivalent muons in each module times the energy loss per module for relativistic muons. Using this energy, particles which pass through the entire spectrometer were grouped in bins and used to construct average integral cascade growth curves. These were done separately for the various charges and plotted on an energy/nucleon basis. Two samples for carbon and iron are shown in figure 3. Our earlier analysis (OBR) was based upon total energy and was not done separately for the different charges. Some differences between the curves can be seen at low energy and small depths. These differences are believed to be due to the importance of ionization loss at low energies. Above 2 GeV/nucleon the curves are quite similar, and so all the data were combined on an energy/nucleon basis to get the series of growth curves shown in figure 4a.

The curves could be expressed as:

$$E_n = E_o \, (1 - \exp(n/\lambda)) \qquad (1)$$

where E_n is the measured energy using n modules and E_o is the energy of the incident particle. $\lambda(E_o)$, the number of modules necessary for absorbing (1-1/e) of the incident energy, was energy dependent. In figure 4b the energy dependence of $\lambda(E_o)$ is shown to increase from 1 to about 6 or 8 modules over the energy range 1 to 100 GeV/nucleon. These empirically fitted curves also give the energy E_o as a function of the measured energy. The correction used to obtain E_o from the data is shown in figure 4c. The spectral exponents derived using the two extreme values of the correction shown in the figure differ by less than half the statistical uncertainty.

The cascades developed by heavy cosmic ray nuclei in the spectrometer were compared with the Monte Carlo calculations of Jones (1971). Our cascade curves agreed, and showed the energy deposit per incident nucleon was essentially indpendent of the charge of the nucleus.

These curves also were used to find the energy of particles escaping out the sides of the spectrometer. These data can be used to double the statistical significance of our results. The data on nuclei exiting through the sides gave spectra 0.1 to 0.2 steeper than particles going through the bottom. However, the differences in spectral exponents between the different nuclear species were approximately the same and the statistical significance was enhanced by including these particles.

The final correction to the data was for the energy going into nuclear disintegration which is not observed by the spectrometer. This energy goes primarily into nuclear excitation, rest energy of the particles produced, and neutrons (Murzin, 1971). This is perhaps the most uncertain portion of the analysis. We have compared the response of the spectrometer to the C response below 2 GeV/nucleon where the C varies sufficiently, and the two methods agree quite well. Most of these particles stop in the spectrometer, and the correction made for nuclear disintegration energy is insignificant. At higher energy, we know from proton calibrations at 10 - 20 GeV/nucleon (Whiteside et al., 1973) that 30 $\pm$5% of the energy was unobservable. This is in agreement with Monte Carlo calculations (Jones, 1971) which have now been compared with many calibration runs with different particles including C and O nuclei at 2.1 GV/c at the Bevatron at Berkeley. Using the Monte Carlo data we correct for a fraction of nuclear disintegration energy which decreases logarithmically from 50% at 1 GeV/nucleon to 20% at 100 GeV/

nucleon. This represents a significant change from our earlier analysis (OBR) in which our corrections were based upon much less information and results in somewhat flatter spectra than those reported previously.

Uncertainties in these corrections leave us with a possible systematic error in our spectral exponents of perhaps $\pm$ 0.1. We believe, however, that the relative spectra are accurate to within the statistical uncertainties. The spectral exponents derived using only the energy deposited in the spectrometer are quite close to the spectra obtained after all corrections have been applied, giving us confidence that our corrections are not introducing distortions in the shape of the energy spectra.

Careful attention to the possible effects due to electronic non-linearities and detector response non-linearities convince us these effects make a negligible contribution. It is planned to check the response of the spectrometer against the response of a gas Cerenkov detector at energies above 10 GeV/nucleon in the near future. This will provide us with an additional handle on the nuclear disintegration correction.

V. RESULTS

The relative abundance observed at the balloon altitude has to be corrected for nuclear interactions in the matter in the telescope (4.5 gm/cm^2) and for interactions in the atmosphere (7.4 gm/cm^2) in order to get an accurate idea of the relative abundance distribution of the primary cosmic radiation. This requires a knowledge of all the fragmentation parameters and their energy dependence. Information on nuclear fragmentation parameters is still incomplete (Cleghorn et al., 1968, von Rosenvinge, 1970). Direct experimental determinations of fragmentation cross-sections using

protons incident on high Z targets have shown that cross-sections are constant to ±10% beyond 1 GeV/nucleon (Shapiro et al., 1971). Though all fragmentation interactions have not been studied completely, variation of cross-section with energy seems to be unlikely.

In extrapolating the observed flux to the top of the atmosphere, we have used the concept of the absorption length $\Lambda_i = \lambda_i / \sum_{j=i} (1-P_{ij}N_j/N_i)$ where λ_i is the interaction mean free path, P_{ij} are the fragmentation parameters for the production of the i^{th} nucleus from j^{th} heavier component, N_i and N_j are the abundances of i^{th} and j^{th} components respectively.

We have used the Λ_i from Webber et al., (1972) to extrapolate the observed flux to the top of the atmosphere.

Table 2 gives the integral flux of the different groups of nuclei at the top of the atmosphere. Also given are the results from other observers for comparison.

TABLE 2

Flux from Different Experiments in Particles/m^2-sec-ster

Group of nuclei	GSFC (>4.5 GV)	Webber et al.	Smith et al. (>5 GV)	Mewaldt et al. (>5 GV)
C+O	3.45 ± .7	4.66 ± 0.14 (>4.35 GV)	4.13 ± .07	
10≤Z≤14	1.08 ± .2		1.5 ± .03	
15≤Z≤23	.30 ± .06		.36 ± .03	
20≤Z≤28	.44 ± .09	.489 ± .02 for Z≥17 (>4.10 GV)		.417 ± .03

Our carbon and oxygen fluxes are low compared to those of other workers. whereas there are no severe discrepancies for the other nuclei. We believe this is related to the background rejection we have discussed above. The

selection results in our losing some genuine events up through oxygen nuclei. The correction for this loss is estimated to be at most 25% for carbon and oxygen and only a few percent for iron. This leaves us with a 35% discrepancy which is probably due to events interacting near the top of the spectrometer which look like background in the charge module.

The energy spectra of various nuclei and groups of nuclei are shown in figure 5. Below 2.0 GeV/nucleon the spectral shape is determined by the geomagnetic cutoff and was time dependent because the balloon drifted from 5.0 GV to 3.2 GV cutoff during the course of the flight. The data were fitted to power law spectra of the form

$$dN/dE = k/E^{\gamma} \quad (E \text{ in GeV/nucleon}) \qquad (2)$$

above 2.0 GeV/nucleon. This energy was chosen in order to be free of geomagnetic cutoff effects.

The data from all the nuclei are summarized in table 3. The exponents have been obtained using a least squares fitting technique. Five energy bins per decade were used giving a bin width comparable to the energy resolution. The table also gives the χ^2 and the degrees of freedom for the fitted spectrum and the number of counts on which it is based. We believe that the difference in the spectral indices of the different species are known with greater confidence than the absolute value of the exponents of any nuclear species due to the systematic effects discussed.

The H and He spectra are from data taken above 50 GeV total energy (Ryan et al., 1972). Some of the differences in exponent between these and the heavier nuclei reflect a general flattening of the H and He spectra below 10 GeV/nucleon, probably due to solar modulation.

TABLE 3

Nuclei	γ	Σ	Degrees of Freedom	Number of Events Included	Number of Particles Above 20GeV/Nucleon	Correction Factors For Flux*
H	$2.75\pm.03$					
He	$2.77\pm.05$					
Li	$2.28\pm.15$	3.2	6	122	2	(1.25)(1.12)(1.13)
Be	$2.6\ \pm.2$	4.1	4	121	0	(1.25)(1.14)(1.13)
B	$2.76\pm.13$	2.2	5	229	3	(1.25)(1.16)(1.13)
C	$2.52\pm.06$	13.2	7	881	25	(1.25)(1.17)(1.27)
N	$2.73\pm.11$	7.3	6	299	5	(1.25)(1.19)(1.24)
O	$2.57\pm.06$	7.2	7	783	25	(1.25)(1.21)(1.30)
B+N	$2.77\pm.08$	4.1	6	528	8	$(1.25)(1.17)(1.19\pm.05)$
C+O	$2.56\pm.04$	14.0	7	1664	50	(1.25)(1.19)(1.27)
10-14	$2.44\pm.07$	.8	7	529	18	(1.15)(1.25)(1.32)
15-23	$2.1\ \pm.2$	1.3	5	140	3	(1.0)(1.33)(1.38)
Fe group	$2.0\ \pm.14$	2.4	5	99	5	(1.0)(1.45)(1.66)
all $Z\geq3$	$2.55\pm.03$	16.4	8	3207	88	(1.2)(1.2)(1.27)

Geometric factor = $1420 cm^2$ ster sec

*(correction for events outside identification limit) (correction for interactions in charge module) (correction for atmospheric attenuation)

The exponents of the energy spectra of the secondary nuclei B and N are larger than those of C and O. The exponents of the heavy nuclei are considerably flatter. The spectra of Li and Be have been recovered from a region of very large background, and so our confidence in these spectra is much less. Their flatter spectra are characteristic of spectra with background contamination.

The ^{2} values indicate that for the most part power laws are reasonable representations of the data. The spectral exponents agree well with those of Smith et al., (1973) using a magnetic spectrometer.

VI. DISCUSSION

Our result that the B+N spectrum is steeper than the spectrum of C+O is qualitatively consistent with the differences between L and M nuclei previously reported: Webber and Ormes (1967), Smith et al., (1973), and Webber et al., (1973). The data all indicate the spectra of secondary nuclei are steeper than those of primaries in agreement with Smith et al., (1973) and Juliusson et al., (1972). We believe that the decrease in the secondary/primary ratio is gradual and represents a power law difference of about 0.2 in spectra, and does not indicate the precipitous drop seen by Juliusson et al. At these energies the fragmentation parameters are expected to be independent of energy, and so it is natural to follow Smith et al., in interpreting this result in terms of an energy dependence to the residence time in the interstellar medium. In this case the lifetime probably decreases by a factor of 2 or 3 between 1 and 100 GeV/nucleon making the leakage length about 2 gm/cm^2 at 100 GeV/nucleon. If the leakage length does decrease faster than this, i.e. to a few tenths of a gm/cm^2 by 100 GeV/nucleon (Webber et al., 1973) then there will be severe difficulties with galactic models in

explaining the isotropy of underground muons from cosmic rays at 10^{12}eV (Elliot et al., 1970, Audouze and Cesarsky, 1973).

We believe (Ormes and Balasubrahmanyan, 1973, Ramaty et al., 1973) that the difference between the Fe and C+O spectra is too large to be explained as a propagation effect as attempted by Webber et al., (1973). This difference in interpretation is in part related to experimental differences in the data from the secondaries produced by spallation of iron. It can only be resolved by further experimentation. If the differences are related to the acceleration mechanism, it may be due to either separate sources (either location or type) or to Z dependent forces on the particles. By measuring the spectra of Ne, and Si we should be able to resolve this question. Our spectra of the 10 to 14 group are consistent with having the same spectrum as the C+O within statistical uncertainties.

The spectral exponents of secondaries are steeper than those of the primaries in these energy ranges, which suggests an energy dependent breakdown of the trapping of these nuclei either in source regions or in the interstellar medium. If the flatter iron spectrum can be explained by propagation, the spectral exponent should steepen at high energies as the leakage length becomes shorter.

The results reported in this paper represent the first use of an ionization spectrometer for the study of the energy distribution of heavy nuclei. Due to the limited exposure in the balloon flight, the data at high energy have statistical limitations. In the energy range over which most of the data has been collected (2 to 10 GeV/nucleon) there have been appreciable corrections due to the nuclear disintegration energy not seen

by the spectrometer. So far we have not been able to calibrate the response of the spectrometer to complex nuclei by another independent technique. We are planning to get some checks on the energy measurement using a gas Cerenkov counter in a future flight. But in spite of the limitations of this data, it is already clear that there are many interesting changes in the composition of cosmic rays at high energies. These results point to the existence of a fertile field for experimental observations in the energy region beyond a few GeV/nucleon. For example, new results from the Chicago group (Juliusson and Meyer, 1973) indicate that the C/O ratio also varies above 30 GeV/nucleon.

We should also remark that the other techniques which work in the range 1 to 100 GeV/nucleon, such as gas Cerenkov detectors and magnetic spectrometers have their limitations, and minor differences in the results are to be expected. In principle the spectrometer techniques should be best suited to the energy range 10 to 10^4 GeV/nucleon where particles are so rare that satellite observations of a year or more duration will be required to obtain statistically significant results.

Future cosmic rays experiments in satellites should be able to resolve differences in interpretation of the data by being able to detect anisotropies, slight spectral discontinuities, and other small differences in composition which may be missed by balloon experiments with their limited observing times. In any case we feel that the high energy composition experiments in the several 100 GeV region will give information crucial to the understanding of cosmic ray sources, acceleration phenomena, and propagation.

ACKNOWLEDGEMENT

We would like to express our appreciation to Dr. F. B. McDonald for his encouragement and support of this research. We have been greatly stimulated by discussion of these results with Dr. R. Ramaty and with Professor W. R. Webber.

We are greatly indepted to the engineering, technical, and data analysis personnel who have devoted long hours to make these results possible. Our thanks also go to Drs. M. J. Ryan and J. F. Arens for their contributions to this work.

REFERENCES

Akimov, V. N., Fetisov, I. N., Morozov, A. E., and Slavatinsky, S. A., 1970, Acta Physica Hung., 29, Suppl; 3, 231.

Audouze, J. M., and Cesarsky, C. J., 1973, Nature, 241, 99.

Cleghorn, T. F., Freier, P. S. and Waddington, C. J., 1968, Canadian J. Phys., 46, 5572.

Elliot, H., Thambyahpillai, T., and Peacock, D. S., 1970, Acta Physica Hung., 29, Suppl., 1, 491.

Jones, W. V., Pinkau, K., Pollvogt, U., Schmidt, W. K. H., and Huggett, R. W., 1969, Nucl. Inst. and Methods, 72, 173.

Jones, W. V., 1971, Proc. 12th Intl. Conf. Cosmic Rays, Hobart, 1, 190.

Juliusson, E., Meyer, P., and Muller, D., 1972, Phys. Rev. (Letters) 29, 445.

Juliusson, E., and Meyer, P., 1973, Bull. A. P. S., 18, 540.

Murzin, V. S., 1971, Progress in Cosmic Ray Physics (Amsterdam: North Holland).

Ormes, J. F., Balasubrahmanyan, V. K., McDonald, F. B., and Price, R. D., 1968, I.E.E.E. Trans. Nucl. Sci. NS-15, 3, 566.

Ormes, J. F., Balasubrahmanyan, V. K., 1970, Acta Physica Hung. 29, Suppl. 4, 397.

Ormes, J. F., Balasubrahmanyan, V. K., and Ryan, M. J., 1971, Proc. 12th Intl. Conf. Cosmic Rays, Hobart, 1, 178.

Ormes, J. F., and Balasubrahmanyan, V. K., 1973, Nature, 241, 95.

Ramaty, R., Balasubrahmanyan, V. K., and Ormes, J. F., 1973, Science, 180, 731.

Ryan, M. J., Ormes, J. F., and Balasubrahmanyan, V. K., 1972, Phys. Rev. (Letters), 28, 985.

Shapiro, M., and Silberberg, R., and Tsao, C. H., 1971, Proc. 12th Intl. Conf. Cosmic Rays, Hobart, 1, 221.

Silverberg, R. F., Ormes, J. F., and Balasubrahmanyan, V. K., 1973, Submitted to J. Geophys. Res.

Smith, L. H., Buffington, A., Smoot, G. F., Alvarez, L. W., and Wahlig, W. H., 1973, Ap. J., 180, 987.

von Rosenvinge, T. T., 1970, Ph.D. Thesis, University of Minnesota.

Webber, W. R., and Ormes, J. F., 1967, J. Geophys. Res. 72, 5957.

Webber, W. R., Damle, S. V., and Kish, J., 1972, Astrophys. and Sp. Sci., 15, 245.

Webber, W. R., Lezniak, J. A., Kish, J. C., and Damle, S. V., 1973, Nature, 241, 96.

Whiteside, H., Crannell, C. J., Crannell, H., Ormes, J. F., Ryan, M. J., and Jones, W. V., 1973, Nucl. Inst. and Methods, in Press, GSFC X-661-72-316.

FIGURES

Figure 1: Schematic diagram of the balloon flight experiment.

Figure 2: Charge histogram obtained from 4 parameter charge analysis. Pulse height scale is normalized to 36 for carbon.

Figure 3: Integral cascade growth curves for carbon and iron nuclei. Curves are similar on an energy/nucleon basis.

Figure 4: Integral cascade growth curves for all nuclei are fitted to give the absorption length and thus the energy incident on the spectrometer.

Part a) Integral growth curves for all nuclei. The crosses represent the asymptotic energy and the numbers next to the crosses are λ^{-1}. The number of events on which these average curves are based are also given.

Part b) The absorption mean free path as a function of energy.

Part c) The correction factor giving the incident energy from the measured energy as a function of the measured energy. The correction used was the more extreme curve. Using the less extreme curve changed the spectral exponents by less than the 1 σ statistical uncertainty.

Figure 5: Energy spectra of various nuclei and groups of nuclei. The most obvious spectral differences are between C+O and Fe. Data below 2 GeV/nucleon are affected by geomagnetic cutoff.

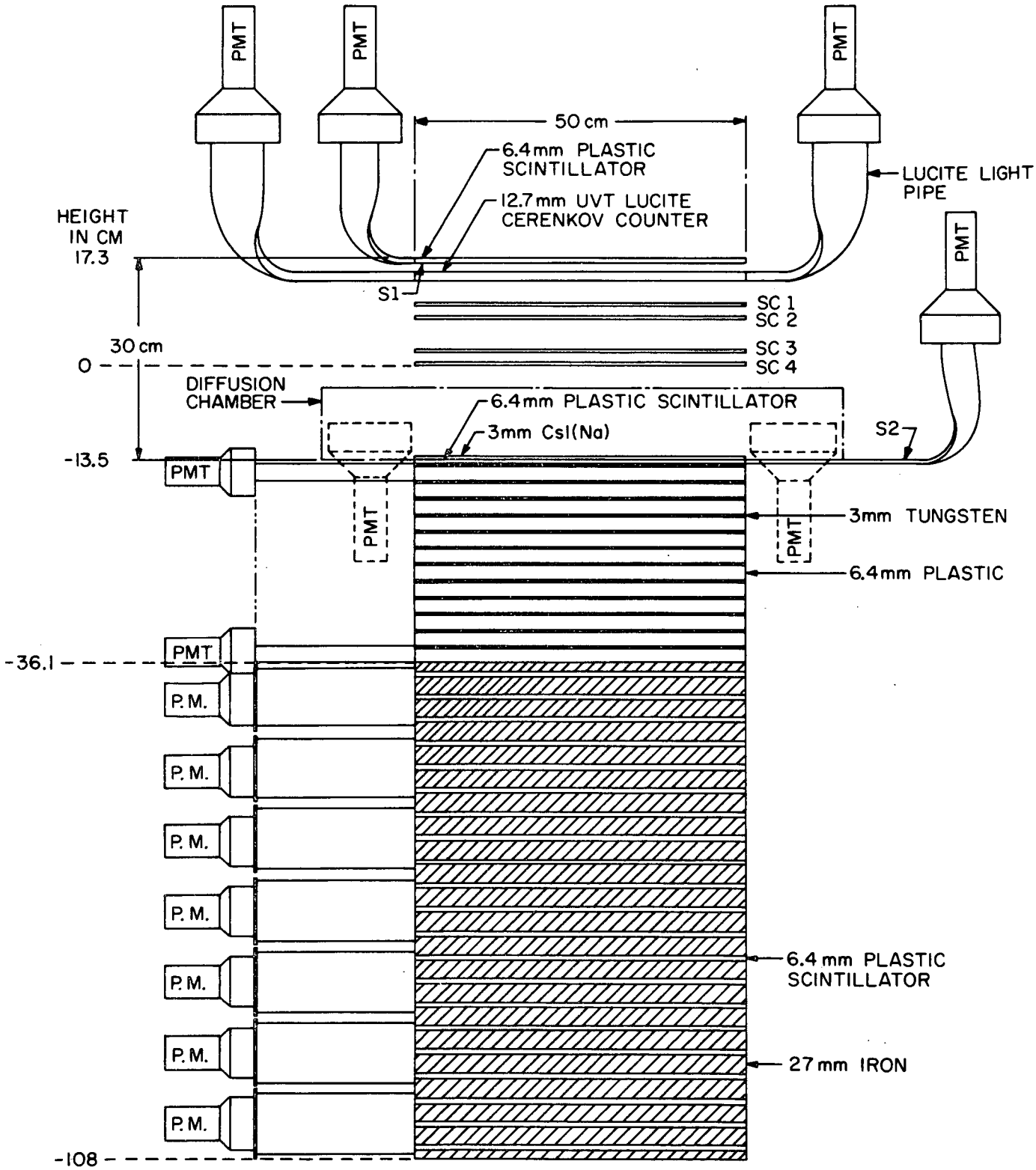

Figure 1

IONIZATION SPECTROMETER

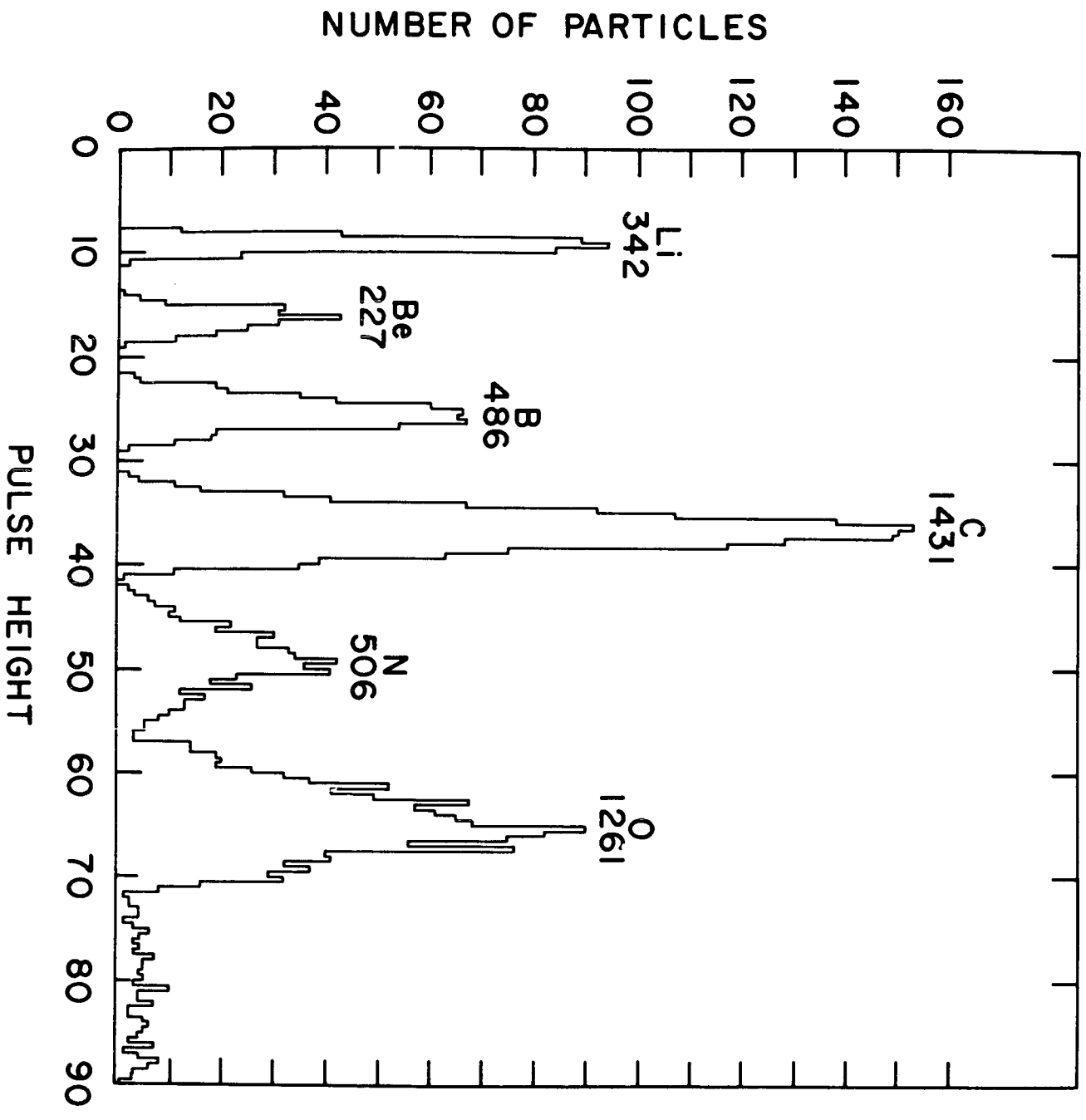
NUMBER OF PARTICLES
0
20
40
60
80
100
120
140
160
PULSE HEIGHT
0
10
20
30
40
50
60
70
80
90
Li
342
Be
227
B
486
C
1431
N
506
O
1261

Figure 2

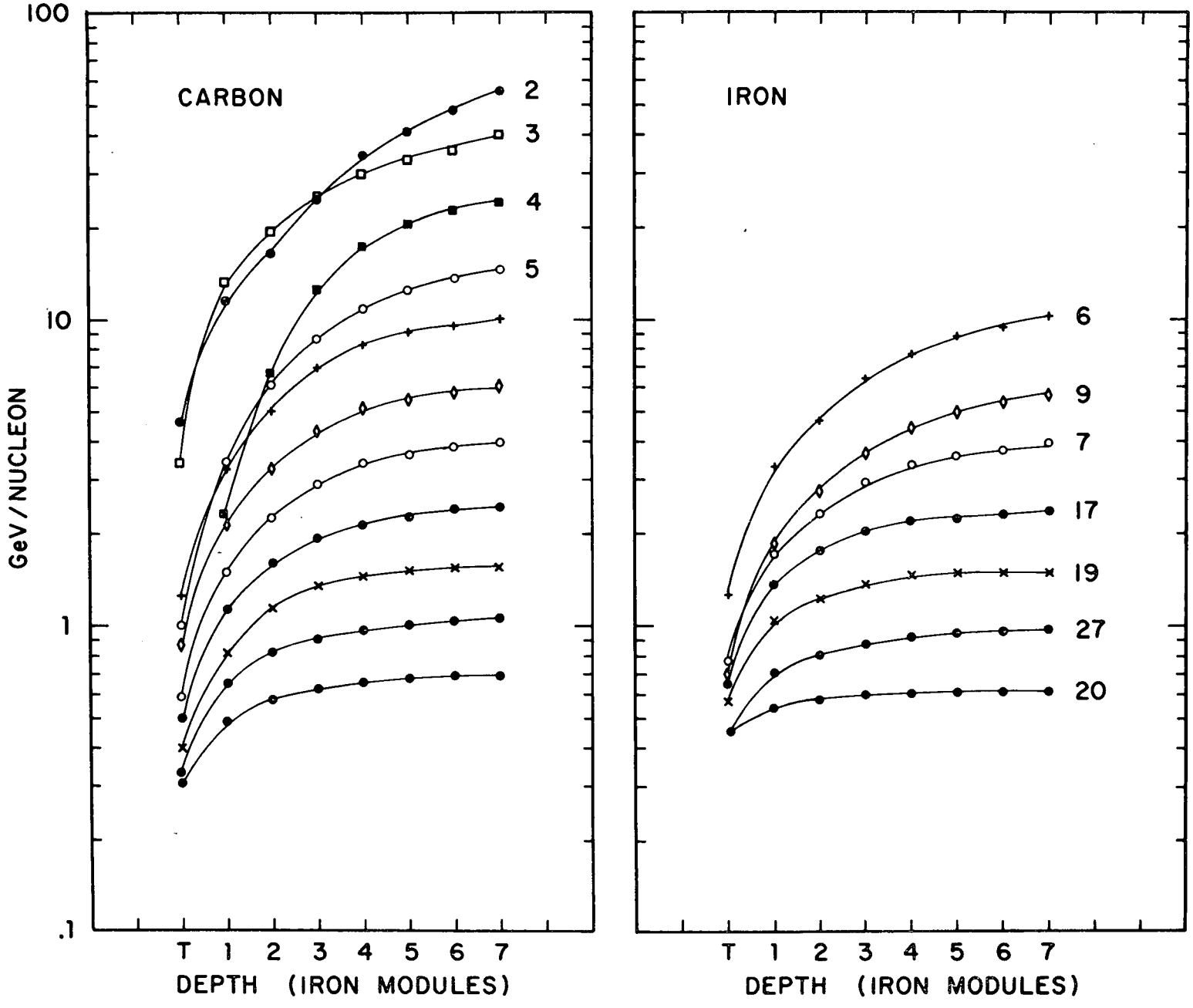
100
10
1
.1
GeV/NUCLEON
CARBON
2
3
4
5
6
9
7
17
19
27
20
T 1 2 3 4 5 6 7
DEPTH (IRON MODULES)
IRON
T 1 2 3 4 5 6 7
DEPTH (IRON MODULES)

Figure 3
26

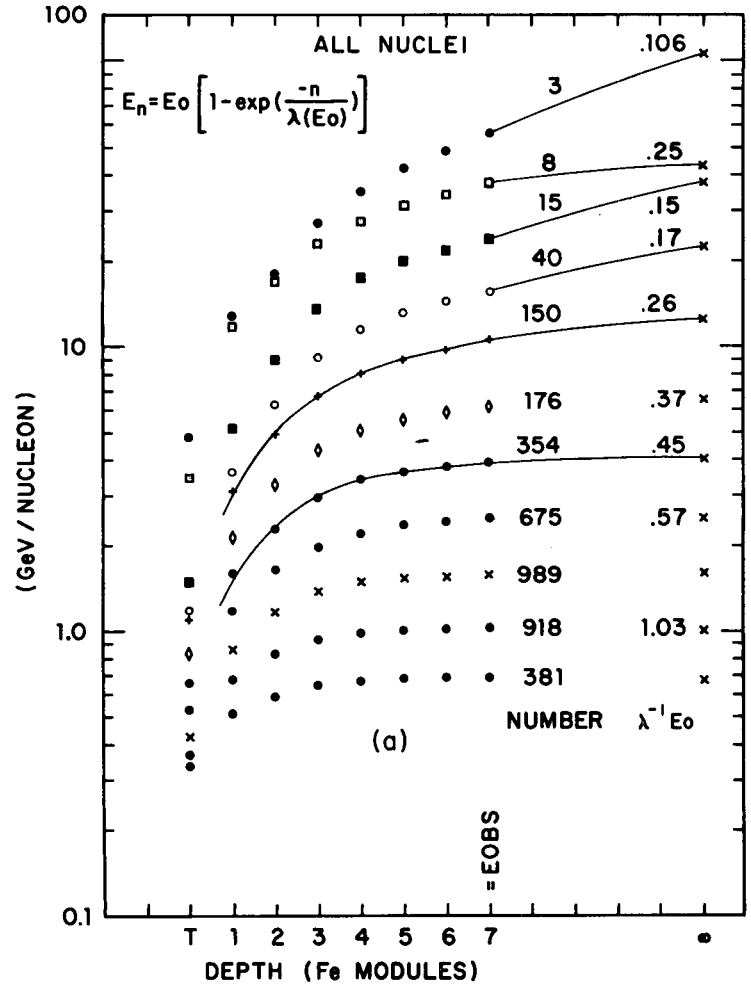
ALL NUCLEI
$E_n = E_o\left[1-\exp\left(\frac{-n}{\lambda(E_o)}\right)\right]$
3
8
15
40
150
176
354
675
989
918
381
.106
.25
.15
.17
.26
.37
.45
.57
1.03
NUMBER $\lambda^{-1}E_o$
(a)
=EOBS
(GeV / NUCLEON)
DEPTH (Fe MODULES)
T 1 2 3 4 5 6 7 ∞
100
10
1.0
0.1

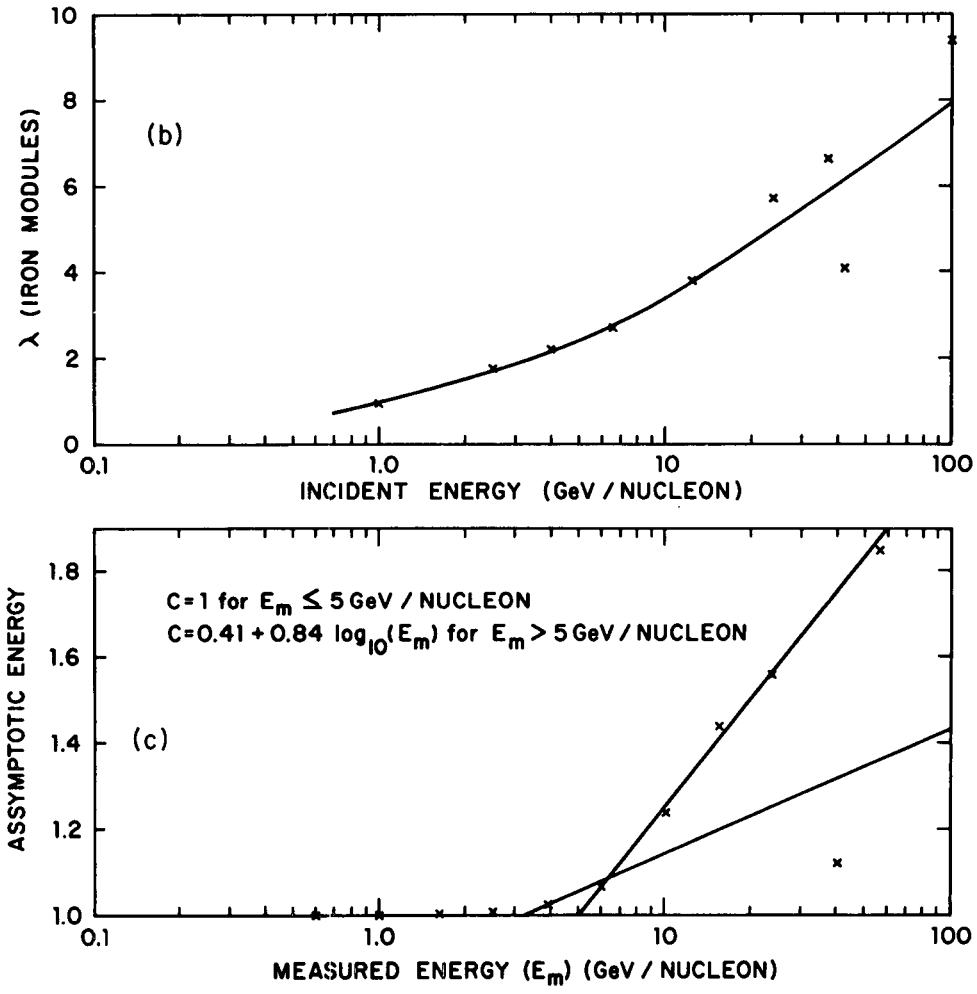
(b)
λ (IRON MODULES)
INCIDENT ENERGY (GeV / NUCLEON)
(c)
C=1 for $E_m \leq 5$ GeV / NUCLEON
C=0.41 + 0.84 $\log_{10}(E_m)$ for $E_m > 5$ GeV / NUCLEON
CORRECTION FACTOR TO GET ASSYMPTOTIC ENERGY
MEASURED ENERGY (E_m) (GeV / NUCLEON)

Figure 4

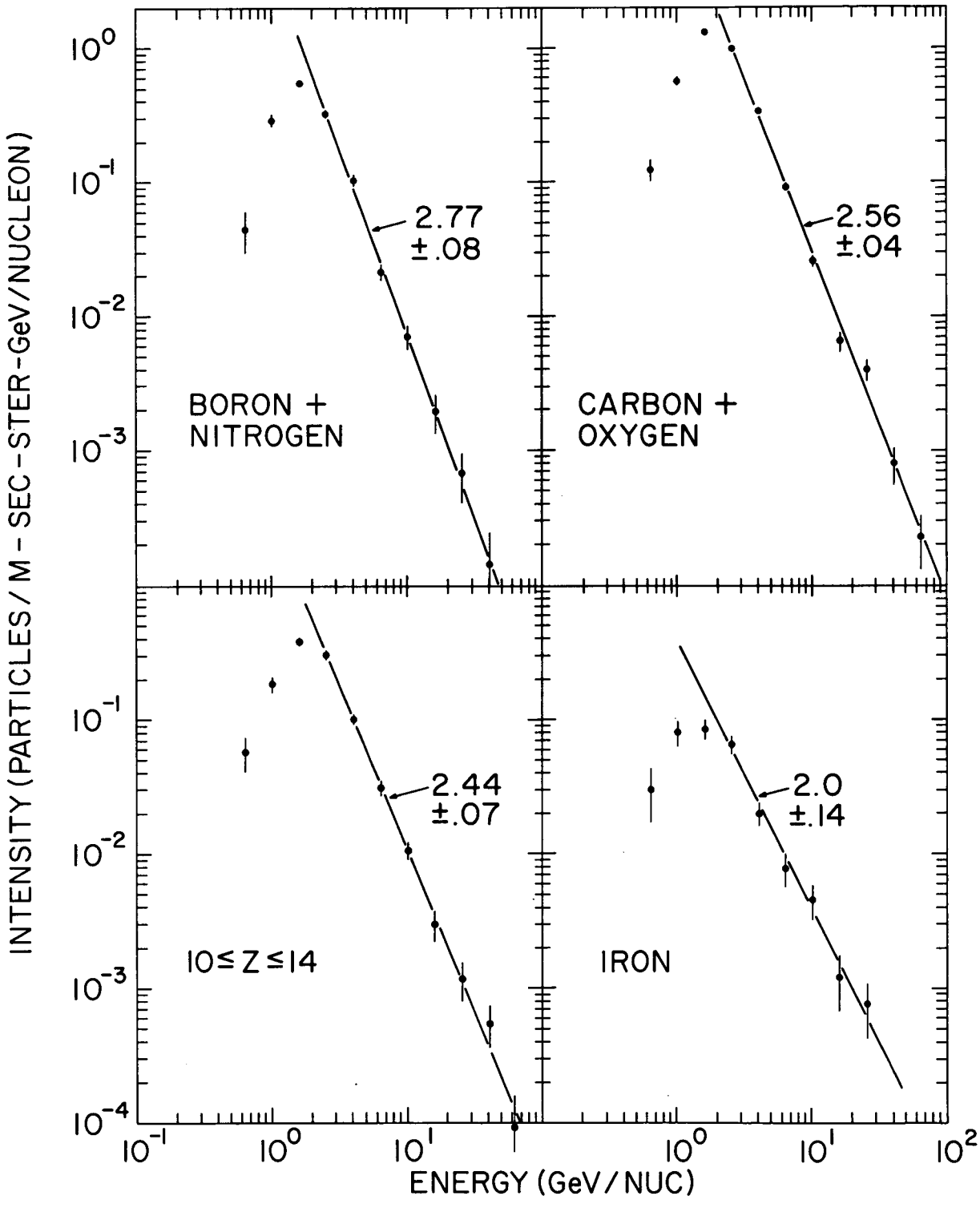
INTENSITY (PARTICLES / M - SEC - STER - GeV/NUCLEON)
ENERGY (GeV/NUC)
BORON + NITROGEN
2.77 ±.08
CARBON + OXYGEN
2.56 ±.04
10≤Z≤14
2.44 ±.07
IRON
2.0 ±.14

Figure 5